Available online at www.sciencedirect.com
ScienceDirect
Corrosion Science 49 (2007) 2329–2350
CORROSION SCIENCE
www.elsevier.com/locate/corsci

Effect of atmospheric pollutants on the corrosion of high power electrical conductors – Part 2. Pure copper

Rosa Vera [a], Diana Delgado [a], Blanca M. Rosales [b,*,1]

[a] *Corrosion Laboratory, Institute of Chemistry, Pontificia Universidad Católica de Valparaíso, Chile*
[b] *CIDEPINT, Av. 52 s/n, entre 121 y 122, B1900AYB, La Plata, Argentina*

Received 8 September 2006; accepted 9 October 2006
Available online 17 January 2007

Abstract

The research work performed during this study was simultaneously followed with another one published in this journal as Part I. A1 and 6201 A1 alloy. Its aim was to reveal a comparative picture of the joint effect of marine and industrial atmospheric pollutants on the corrosion resistance of wire metals employed for electric transmission conductors. Weight loss after 4, 11, 16 and 24 months exposure was determined and morphology of the attack analysed through SEM–ESEM–EDX. Cu corrosion products showed higher protectiveness than those of Al in marine sites for the lowest [Cl^-] and in marine-industrial atmospheres even for the highest SO_2 contents. Respect to marine sites where [Cl^-] was higher than [SO_2] Cu was more susceptible than A1.

Keywords: A. Pure copper; B. SEM; B. ESEM; B. EDX; C. Atmospheric corrosion

1. Introduction

Copper and its alloys have traditionally been used as architectural material due to their atmospheric corrosion resistance and the pleasant colours developed on the surface when exposed to the atmosphere (patina), as roofs, monuments, ornaments, etc.

* Corresponding author. Tel./fax: +54 11 4782 9921.
E-mail addresses: rvera@ucv.cl (R. Vera), brosales@fibertel.com.ar (B.M. Rosales).
[1] Researcher of the Consejo de Investigaciones y Científicas y Técnicas (CONICET).

0010-938X/$ - see front matter © 2006 Elsevier Ltd. All rights reserved.
doi:10.1016/j.corsci.2006.10.031

This metal has also been used for electric conductors due to its high conductivity, reason why it is an important material in communication and electronic industries.

The atmospheric corrosion of copper and its alloys has broadly been studied through natural outdoor exposure as in laboratory. The colours of the corrosion products they form during outdoor exposure are from pink-salmon to dark brown and finally green (patina).

Patina is the result of the chemical interaction of trace contaminant elements in the atmosphere mainly sulfates and chlorides. Its composition and morphology depend on the geographic localisation of the test station, the climatic conditions and the contaminant aggressiveness levels [1,2].

Studies performed by Fonseca et al. [2] on copper exposed in 2 sites in Portugal were initiated in summer and winter seasons, being especially focused the initial corrosion steps. Winter initiated exposures attained higher corrosion levels as compared to those initiated in summer.

The copper weathering chemistry and associated mechanisms have been quite well studied. Nassau et al. [3–5] have identified on Cu patinas formed in the atmosphere the following main compounds: cuprite, Cu_2O, brochantite, $Cu_4SO_4(OH)_6$, antlerite, $Cu_3SO_4(OH)_4$, ponsjankite, $Cu_4SO_4(OH)_6 \cdot H_2O$, atacamite, $Cu_2Cl(OH)_3$.

In a study about the influence of the season variations (air temperature and relative humidity) on copper corrosion products, especially for short exposure periods as few months, Zhang et al. [6] reported changes in composition of the patinas obtained. Similar studies performed by Watanabe [7] in three test sites of Tokyo during 1 month in summer and in winter, found that cuprite and ponsjankite were formed on copper exposed in summer, having on the contrary only identified cuprite, when the exposition test was initiated in winter. The corrosion products formed were the same in all 3 exposition sites for both initiation seasons.

Studies performed by Leuenberger-Minger [8] in Switzerland during 4 years on copper, steel and zinc demonstrated that diminution of environmental SO_2 due to environmental protection measures evidenced the relative importance of other atmospheric contaminants, as ozone or nitrogen oxide, on the corrosion of metallic materials.

In the present work various interesting differences in the material as well as in the atmosphere were involved as compared to most atmospheric corrosion studies. Copper was exposed as wires instead of flat samples, having thus determined increased corrosion rates [9], the atmospheres contained from very low urban to very high industrial SO_2 pollutant contents, as well as from coastal highly Cl^- polluted to soft marine atmospheres, combined in natural environments in 17 different proportions. The test periods were long enough to allow data registering since the nucleation step to the attack propagation, providing results able to clarify the patina formation mechanism.

2. Experimental

Selection of the 17 marine and marine-industrial test sites were this study was performed involved very different distances to the pollutant sources. Test stations were installed at distances ranging from 60 m to 4000 m to the sea, between 500 m and 1500 m from an industrial plant, the only SO_2 pollutant source, and different altitudes from 0 to 180 m over sea level (osl).

Tests samples were 99.0% Cu, as received stranded wires of 2.50 mm diameter, cut to 1000 mm length. The specimens were formed as open helixes around a 24 mm diameter mandrill. Crevice by contact with other material or with adjacent spires was avoided. Two replicates of each material were exposed at the outdoor atmospheres, fixed by their isolated ends at 45° angle to the horizon, during 4, 11, 16 and 24 months.

Pollutant concentrations, meteorological parameters and the corrosivity classification of the atmospheres are included in Table 1. The methodology for the atmospheric characterisation and weight loss determinations followed ISO 9223 to 9226 [10–13] and ISO 8407 [14] standards, respectively.

Morphology in plan and in polished cross-section after the tested wires expositions were analysed through scanning electron microscopy using a SEM Philips 515, coupled to an EDAX 9100 analyser for elemental characterisation and an environmental ESEM-EDAX Philips XL 30.

X-ray diffraction analysis was applied to the corrosion products formed after different periods in both types of test sites. A SIEMENS D 5000 with Cu Kα radiation and a graphite monochromator 40 kV/30 mA, in the scanning range 05–70°, were used.

Electrochemical polarisation was applied to weathered copper samples from marine sites 2 and 27 and from the marine-industrial sites 5 and 9 as compared to non-exposed bare Cu witness. The anodic curves were obtained in 0.1 M Na_2SO_4 electrolyte after solution deaereation by 99.99% N_2 bubbling and cathodic ones in air saturated solutions, at 100 mV min^{-1} potential scan rate with constant magnetic stirring. A conventional Pyrex glass cell with Pt counter electrode and a saturated calomel electrode as reference, through a Luggin capillary, were used.

Table 1
Location and ambient characteristics of the 17 test sites

Type of atmosphere	Station (N°)	Exposure site	Sea dist. (m)	Height osl (m)	$[Cl^-]$ (mg m^{-2} d^{-1})	ISO Cat.[a]	$[SO_2]$ (mg m^{-2} d^{-1})	ISO Cat.[a]
Marine	18	Concón	2190	25	17.2	S_1	19.1	P_1
Marine	6	Concón	4060	25	17.4	S_1	29.8	P_1
Marine	20	Reñaca	930	125	19.0	S_1	21.1	P_1
Marine	23	Reñaca	1810	145	21.1	S_1	33.3	P_1
Marine	29	Reñaca	200	125	27.3	S_1	19.2	P_1
Marine	28	Reñaca	0	0	44.5	S_1	9.4	P_0
Marine	24	San Antonio	1051	69	20.1	S_1	1.2	P_0
Marine	12	San Antonio	227	62	21.4	S_1	4.1	P_0
Marine	15	San Antonio	14770	180	22.1	S_1	3.6	P_0
Marine	27	San Antonio	269	21	31.0	S_1	5.1	P_0
Marine	2	San Antonio	4	0	131.8	S_2	7.2	P_0
Marine-Indust.	10	Ventana	760	30	32.0	S_1	86.8	P_3
Marine-Indust.	14	Ventana	1220	41	28.3	S_1	94.4	P_3
Marine-Indust.	4	Ventana	1980	47	18.6	S_1	103.8	P_3
Marine-Indust.	13	Ventana	600	13	17.5	S_1	240.4	$>P_3$
Marine-Indust.	9	Ventana	660	12	21.3	S_1	282.3	$>P_3$
Marine-Indust.	5	Ventana	690	11	20.4	S_1	651.2	$>P_3$

[a] According to ISO 9224 standard [11].

3. Results

The test sites location data, pollutant deposition rates and classification atmospheres according to ISO 9224 standard [11] are displayed in Table 1. The yearly meteorological parameters of the region involving the 17 test sites, temperature (T), relative humidity (RH), predominant winds and rains are shown in Fig. 1a–c as a function of time. The

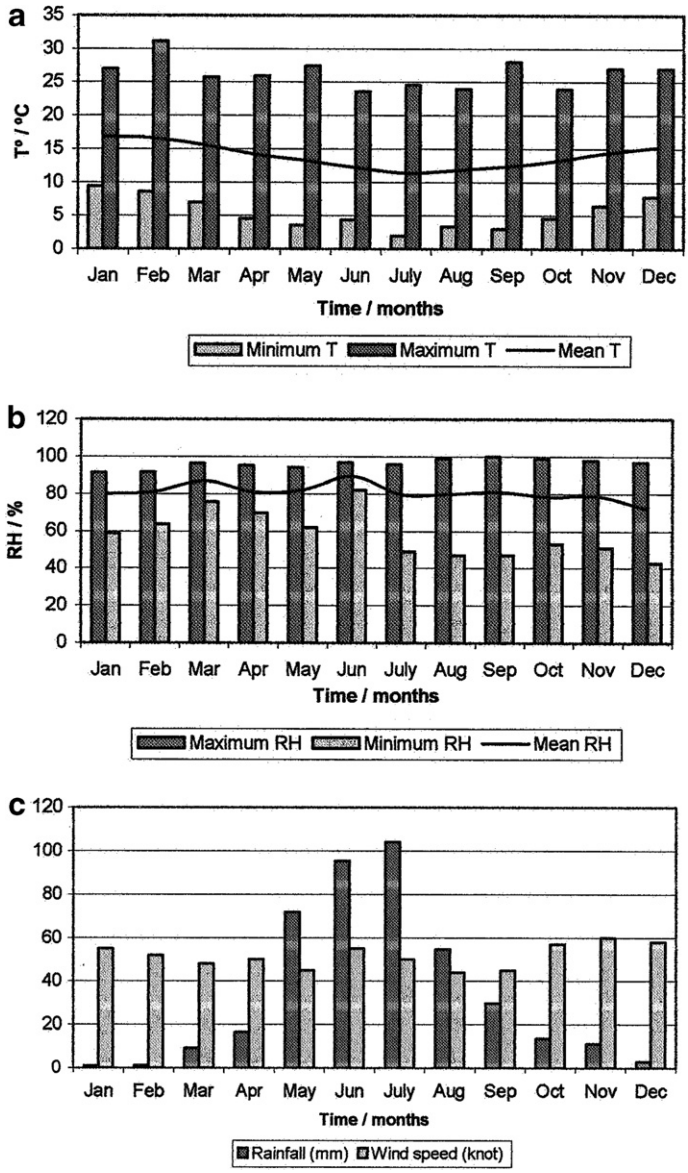

Fig. 1. Meteorological parameters in the Fifth Region, Chile, with time (period 1970–2003): (a) extreme and mean temperature, (b) extreme and mean relative humidity and (c) mean rainfall and maximum wind speed.

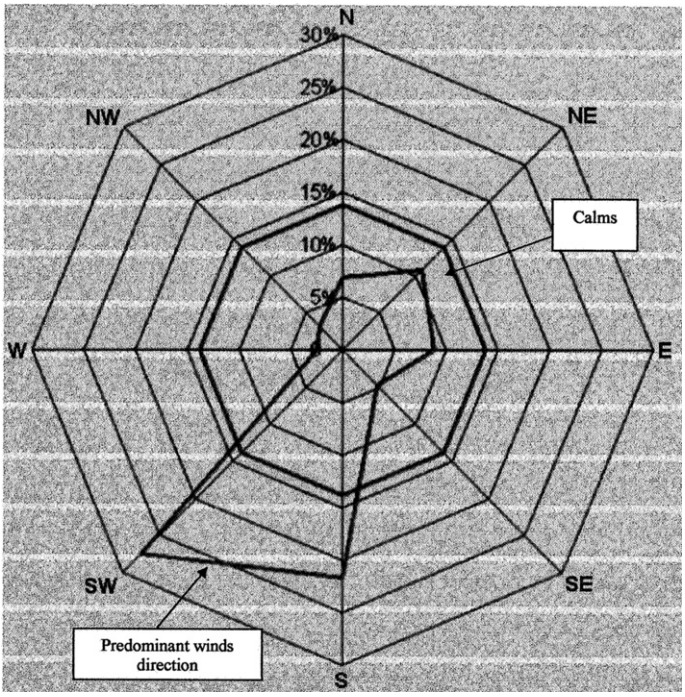

Fig. 2. Traverse board of Valparaiso, Chile.

traverse board of the same area shown in Fig. 2, evidences that SW yearly predominant winds supply of different salt fog amount to the test stations depending on the distance to the sea shore line and more or less free access determined by their height and of the screen effect of obstacles from the coast. Fig. 3 shows a croquis of the Fifth Region seashore zone of Valparaiso, Chile (Lat. 32°S, Long. 71°W) where the test sites were mounted.

The main components of the corrosion products determined through X-ray diffraction are shown in Table 2, do not evidencing significant differences amongst those formed at sites of each type of atmosphere.

Figs. 4 and 5 depict the copper mass loss in function of time at the test sites in marine and marine-industrial environments, respectively.

In Fig. 6 the in plan aspect of samples exposed to marine atmospheres 6 and 2 reveal differences among 4 and 16 month exposure times, including EDX of the respective corrosion products.

In Fig. 7, polished transverse cross-section of Cu can be observed after 4 and 11 month exposure in the sites 5 and 9 of marine-industrial atmospheres with very distinct SO_2 content. It can be noticed the thickness and compactness enhancement with the industrial pollutant and time increases.

Anodic and cathodic polarisation of weathered copper in 0.1 M Na_2SO_4 solution shown in Fig. 8, evidenced different relative behavior of samples after 24 month exposure at the marine test sites 2 and 27, and 11 month at the marine-industrial test sites 5 and 9, as compared to non-exposed samples.

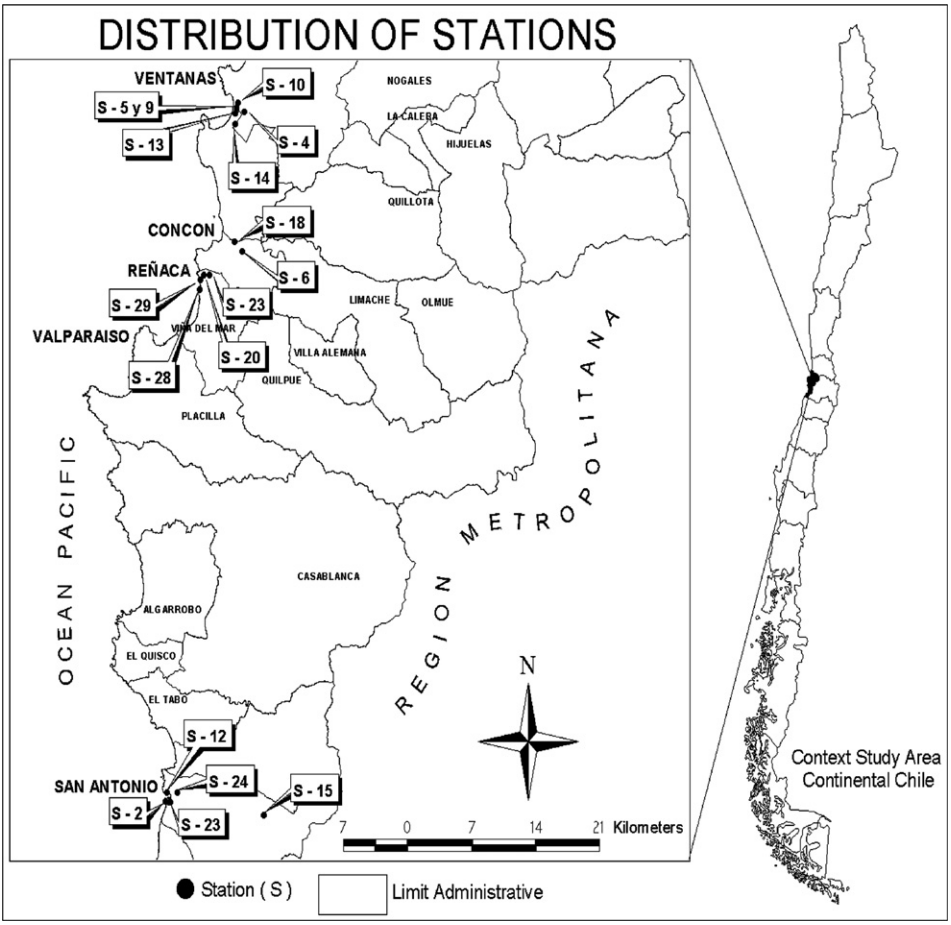

Fig. 3. Croquis of the test stations geographic location.

Table 2
X-ray diffraction of the corrosion products formed on copper in the marine and marine-industrial test sites after different exposure times

Copper	
Marine sites	Marine-Industrial sites
Atacamite ($Cu_2Cl(OH)_3$)	Atacamite ($Cu_2Cl(OH)_3$)
Sodium chloride (NaCl)	Copper iron sulphide ($CuFeS_2$)
Quartz (SiO_2)	Copper chloride (CuCl)
	Quartz (SiO_2)

4. Discussion

As the maximum pollutant [SO_2] is 200 mg m^{-2} d^{-1} for P3 category according to ISO 9225 standard [12], it can be seen from Table 1 that this limit is surpassed in 3 marine-industrial test/sites designed as 13, 9 and 5. Thus, very high corrosion rates could be

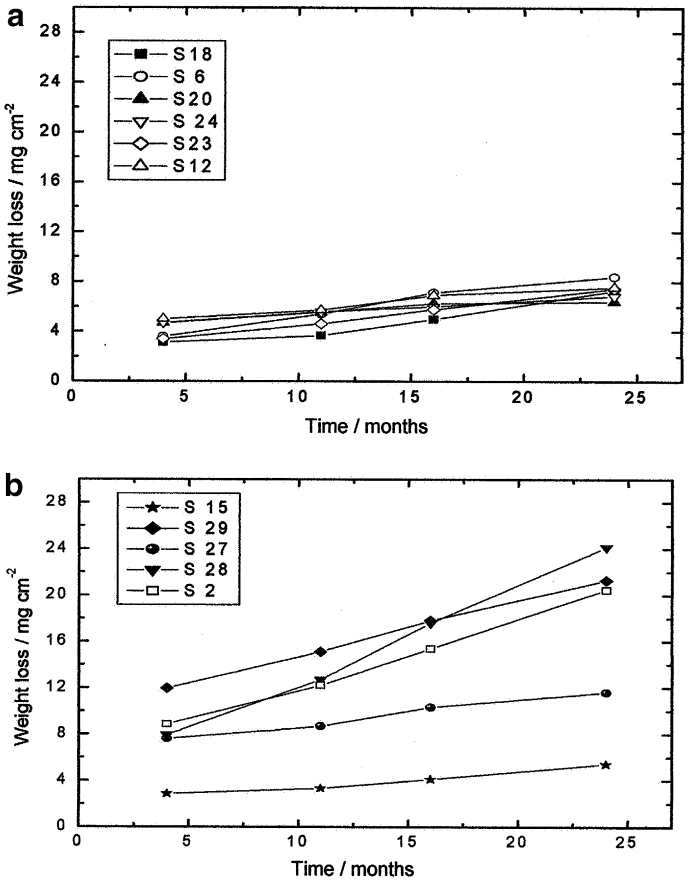

Fig. 4. Mass loss of copper in function of exposure time in marine environments: (a) sites 18, 6, 20, 24, 23 and 12, for lowest Cl^- contents and various SO_2 contents and (b) sites 15, 29, 28, 27 and 2, with higher Cl^- than SO_2.

expected for samples exposed at those sites, as those measured for Al and its 6201 alloy [16].

The many atmospheric contaminant level combinations due to variable distances to pollutant sources, height osl and barrier effects respect to salt fog from the ocean also produce different TOW at the test sites to be considered during the results analysis.

4.1. Weight loss analyses

Good correlation between mass loss and exposure time was always found, while the relationship was not so clear respect to the atmospheric Cl^- and SO_2 deposition rates. In fact, for similar low chloride contents the measured corrosion rates were not always controlled by the SO_2 concentration, as shown in Fig. 4a where almost all sites depicted similar values. Correlation neither was found when higher Cl^- than SO_2 contents were involved, as shown in Fig. 4b for sites 15, 29, 28, 27 and 2, listed according to their Cl^- increasing levels.

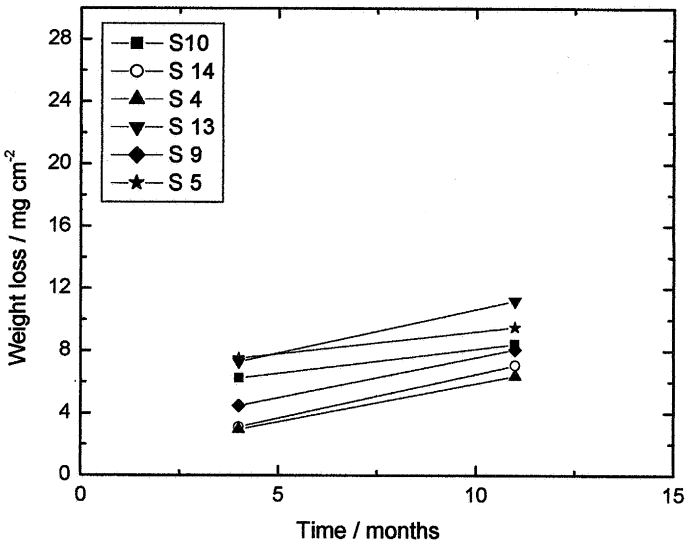

Fig. 5. Mass loss of copper in function of the exposure time in marine-industrial stations, sites 10, 14, 4, 13, 9 and 5, with much higher SO_2 than Cl^- content.

In sites with low SO_2 content the atmospheric aggressiveness was proportional to the Cl^- concentration. Both pollutants synergise the corrosiveness of the atmosphere, having however determined that the highest Cl^- content in site 2 (131.8 mg m^{-2} d^{-1}) does not produce the highest weight loss. On the contrary, site 29 evidences the most intense corrosion on Cu, corresponding to 27.3 mg m^{-2} d^{-1} in Cl^- and 19.2 mg m^{-2} d^{-1} in SO_2. Site 28 with 44.5 mg m^{-2} d^{-1} in Cl^{-1} and 9.4 mg m^{-2} d^{-1} in SO_2 shows a steeper trend as a function of time.

According to these results another very strong factor seems to affect the weight loss data in the test sites: the distance to the sea coast. This factor not only determines de Cl^- deposition rate but it also controls the amount of water in the salt fog reaching the exposed samples. Comparative analysis of Fig. 4a seems to show that most aggressive atmospheres on bare Cu would be associated to the total pollutant content of sites, but the weight loss seems also be proportional to the water available to solubilise the marine and industrial contaminants. Thus, lowest similar values for sites 18 and 23 could be due to the increasing total pollutant amount from the first to the second one, but for almost similar distances to the sea, the higher altitude of 23 would allow more water to reach samples at that place. Sites 6 and 12 show extreme examples of this effect on bare Cu samples, were parameters to compare are total pollutants, distance to the sea and height of the site over sea level (osl). The effect of 47 as compared to 25.5 mg m^{-2} d^{-1} seems to be less effective due to the 4060 vs. 227 m apart from the coast and its 25 vs. 62 m height.

In Fig. 4b higher and more scattered weight loss values allow a better discussion of the same parameters effect. In fact, 15 is the more distant site from the sea shore. Also having quite low SO_2 concentration, it shows for all the test periods the lowest weight losses, that could be attributed to a low time of wetness (TOW) experienced by the samples for a total 25.7 mg m^{-2} d^{-1} total pollutants level. Other considerations allow proposing: (a) the steepest trend for site 28 vs. time, due to the splash effect of the sea water on this site samples,

a

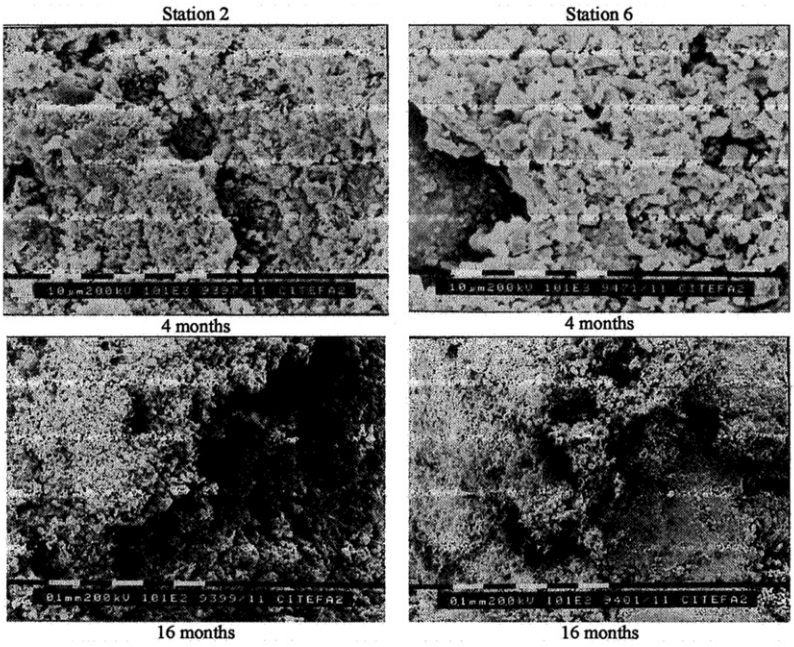

b

ELEM	4 months (WT%)		16 months (WT%)	
	Site 2	Site 6	Site 2	Site 6
Na	4.14	--	3.55	--
Mg	6.17	--	7.28	3.67
Al	12.46	9.27	15.53	36.35
Si	30.71	17.55	45.14	19.76
S	1.26	2.03	0.37	9.82
Cl	7.04	14.27	0.97	0.15
K	2.38	1.03	3.96	0.82
Ca	9.04	0.97	7.73	0.93
Fe	6.33	3.60	11.73	3.51
Cu	19.78	51.29	3.54	25.01
Zn	0.76	--	0.23	--

Fig. 6. Copper samples after 4 and 16 months exposure in the marine environments of sites 2 and 6: (a) SEM aspect and (b) EDX on Cu corrosion products.

a

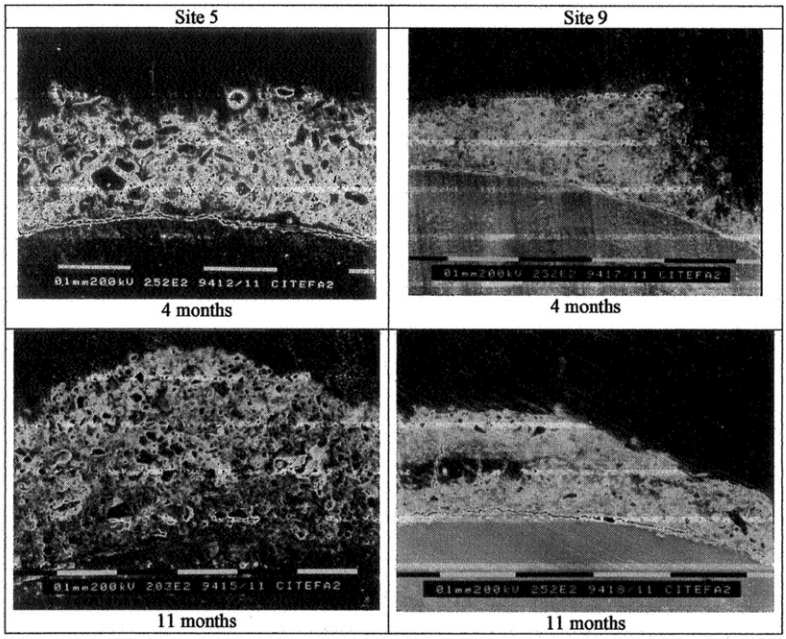

b

ELEM	4 months (WT%)		11 months (WT%)	
	Site 5	Site 9	Site 5	Site 9
Na	10.42	8.45	2.85	4.02
Mg	--	--	2.65	2.15
Al	10.62	6.36	11.55	15.38
Si	5.40	12.74	18.84	20.23
S	14.38	19.01	17.21	15.82
Cl	4.09	1.26	1.57	--
K	0.61	0.43	1.45	1.01
Ca	3.01	8.43	5.51	7.81
Fe	4.84	12.35	11.77	8.79
Cu	37.65	27.83	23.17	19.13
Zn	8.97	3.16	3.46	5.69

Fig. 7. Cross-section of copper samples after 4 and 11 month exposure periods in marine-industrial environments of sites 5 and 9: (a) SEM aspect, (b) EDX on Cu corrosion products, (c) ESEM aspect of copper samples after 11 and 24 month exposure periods in marine environments of sites 2 and 27 and (d) ESEM aspect in cross-section of a pickled copper sample after 11 months exposure in marine-industrial environment of site 5.

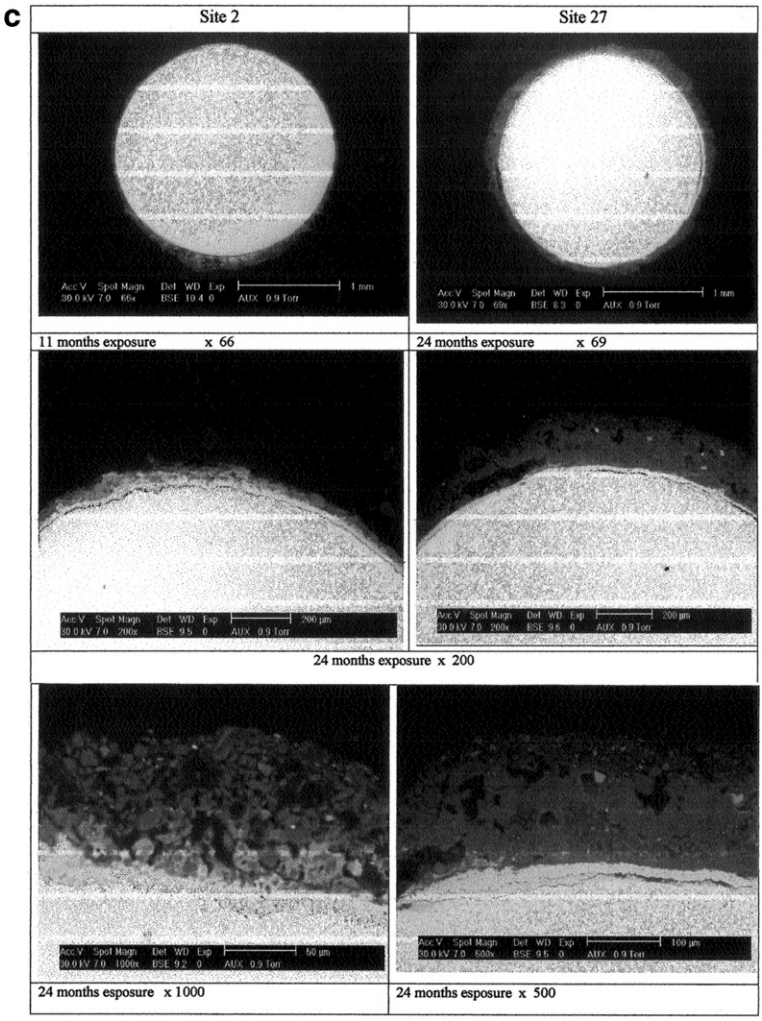

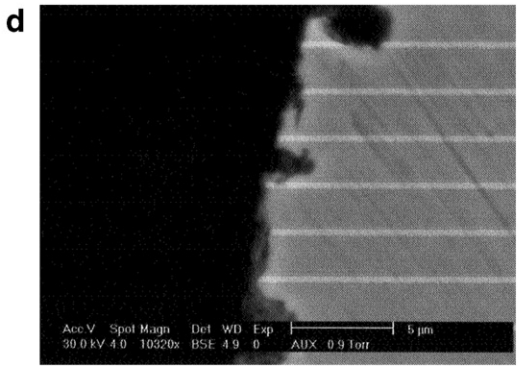

Fig. 7 (*continued*)

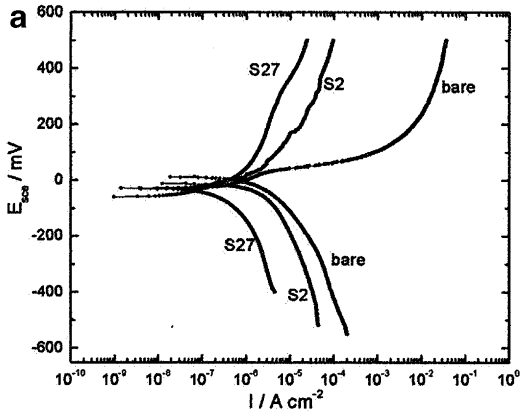

Sample	Ec (mV)	Ic (Acm^{-2})
BareCu	-5.5	7.3×10^{-7}
Site 2	-18	1.8×10^{-7}
Site 27	-24	6.5×10^{-8}

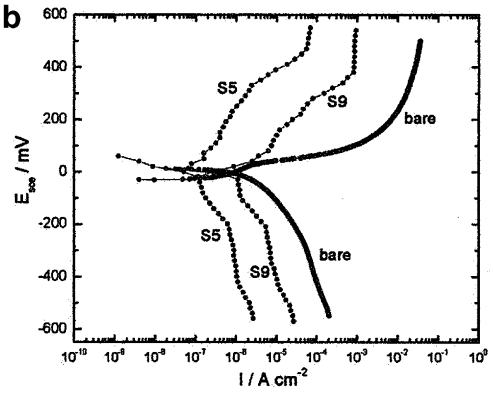

Sample	Ec (mV)	Ic (Acm^{-2})
Bare Cu	-5.5	7.3×10^{-7}
Site 5	-0.84	5×10^{-8}
Site 9	2.29	2.6×10^{-7}

Fig. 8. Polarisation of copper samples after exposure as compared to non-exposed bare Cu, anodic in the absence of oxygen and cathodic in air saturated 0.1 M Na_2SO_4 solution: (a) marine atmospheres of sites 2 and 27 after 24 months exposures and (b) marine-industrial atmospheres of sites 5 and 9 after 11 months exposures.

also causing increased exfoliation as compared to the next site 2, with the highest Cl^- content but 4 m apart from the sea shore, (b) for site 29 it is not clear what could have caused the highest weight loss for the 3 initial periods with only a total 46.5 mg m^{-2} d^{-1} pollutants, in spite of the great water availability at 200 m from the sea shore and 125 m osl which could have avoided most screen effects to the exposed samples, (c) site 27 shows a parallel trend to site 29 vs. time with quite lower weight losses mainly attributable to the almost 100 m lower position osl than 29 and around 15 mg m^{-2} d^{-1} less total contaminant level.

In the marine-industrial stations 10, 14, 4, 13, 9 and 5, with medium chloride levels and SO_2 from high to very high, Cu mass losses showed good correlation with SO_2 atmospheric concentration, as can be seen in Fig. 5. For such SO_2 levels changes in Cl^- concentrations did not show any effect on the atmospheric aggressiveness.

Contrary to the observed in marine test sites in these highly SO_2 polluted test stations after 4 month exposure Cu did not show different weight loss between the two most polluted sites 5 and 9. Being at almost the same distance from the sea shore the TOW seems not being enough to solubilise the whole deposited SO_2 as to make any difference in the liquid phase aggressiveness, even on the bare samples. The same was also observed for the

test sites 14 and 4 and even between 9 and 10 a clear inversion can be noticed for the two first periods.

4.2. Morphology and chemical analyses

Two characteristics rendering analysis of copper corrosion products very interesting are their very low solubility in rain water, main factor promoting patina formation and that most compounds include the environmental pollutants. This later allows copper samples use to assess contamination at the exposure site even when detection is not proportional to the atmospheric content [15,16]. They also retain spurious elements not investigated during the procedures specified for corrosiveness classification according to ISO standards 9223 to 9226.

Morphology and EDX are also connected to the type of atmosphere. EDX analysis performed on corrosion products of different morphology and structural unit size in plan showed that the smooth zones over which more uniform Cu attack was observed had lower environmental pollutant counts. The larger structures presented higher pollutant contents and were associated to deeper localised cave like attacks. The caves were wider and deeper according to the pollutant nuclei size. Such aspect can be appreciated in the different cross-section micrographs, as Cl^- and SO_2 stimulate the localised attack becoming part of the insoluble corrosion products they form on the metal. Cave depth, appreciated in cross-section micrographs evidenced a faster increase with exposure time especially in sites associated to highest Cl^- and SO_2 pollutant content.

When comparing morphology and EDX surface analysis of Cu samples for increasing exposure periods, only a density increase in the globular corrosion products can be observed. Comparable structure sizes resulted from similar overall concentrations of the different pollutants at the test stations, as observed by comparing the weight loss with the respective EDX results. For micrographs corresponding to increasing exposure time at given environments parallel increases were detected in surface globular structures density. Cross-section micrographs showed from scarce, shallow caves and films of poorly cohesive corrosion products to deep attack and highly compact products film in low and heavily polluted atmospheres, respectively.

In marine atmospheres with the highest additional SO_2 contents good correlation was found between particle size of the products formed and grain size of the underlying metal, consistent with in-depth attack propagation through grain boundaries. This attack propagation mechanism, leading to metal grain detachment by exfoliation, would explain the highest slope of weight loss vs. time in Fig. 4b for samples exposed to sites 28 (sea water splash area) and 2 (highest Cl^- deposition rate) respectively, due to grain loss additional to corrosion products dissolution during pickling.

As basic copper chloride and sulphate formation occur, Cl and S mapping of weathered samples in cross-section allowed determining their uniform distribution in the globular corrosion products, characteristic of those formed in the explored atmospheres. Cross-section micrographs in Fig. 7a and c reveal the localised nature of attacks, originating globular structures surrounded by flat areas with soft uniform attack. These two types of regions correspond to brighter and dark areas, respectively, of the in-plan micrographs shown in Fig. 6. Both S and Cl mapping taken on the corresponding $\times 100$ micrographs demonstrated that the uneven morphology produced is associated to heterogeneous pollutant deposition.

4.2.1. In plan analyses

In spite of the generalised concept about the uniform penetration of the atmospheric corrosion this is a concept limited by the magnification applied to observation. In the morphology analysis always localised attacks are found associated to material heterogeneities or to uneven atmospheric material deposition (solid pollutants, water condensation, rain off, etc.).

The products formed also unevenly contribute to the attack nucleation and further propagation, not only spreading on the surface but also in deepness. Once anodic and cathodic sites become defined on the original bare surface their alternance during successive wetting and drying cycles is known to cause an almost uniform attack penetration. However, once corrosion products accumulate, preferentially on the anodic sites, polarisation of those sites favour the establishment of new anodic sites where previously cathodic reactions occurred. Those new anodic sites will led to anodic metal dissolution, but through a thickening film with time. As the product accumulation grows on the originally cathodic areas, the referred alternance will slower the attack penetration throughout the whole surface, leaving a small pick to valley macroscopic roughness even to the naked eye. In coincidence with decreasing mass loss, less intense attack produce decreasing penetration rate becoming the outer corrosion products film thinner and increasingly uniform with time.

Below the whole surface covered by corrosion products this uneven metallic attack will be partially masked, except whether the products are eliminated during acid pickling. The difference among crests and valleys of the corroded surface increases with the atmosphere pollutant content and with the exposure time, as also do the corrosion products thickness. The metal surface roughness only becomes evident after pickling.

Comparative SEM aspect of Cu samples after exposure during 4 and 16 month to the heaviest marine environment of site 2 and medium Cl^- and SO_2 pollutant levels of site 6, shown in (Fig. 6), are in good agreement with the respective weight losses. Larger amount and roughness of corrosion products film on samples of site 2 than 6 can be noticed after both exposure periods, especially for the longest period and low magnification.

The attributed macroscopically uniform atmospheric corrosion of metals can be appreciated on copper when observed in polished cross-sections as those shown in Fig. 7a and c, even when the samples are observed with as high as 200–1000 magnification. Heavily contaminated atmospheres generally originate localised attacks, with initial isolate pitting, surrounded by intact areas of the metal in-between, as those shown in Fig. 7d.

4.2.2. Transverse cross-section analyses

The SEM aspect in polished transverse cross-section after 4 and 11 months exposure in the most aggressive marine-industrial atmospheres of sites 5 and 9 evidence the relative corrosion rates through the corrosion product thickness and texture of the attacked wires shown in Fig. 7. The initial pits propagated with exposure time through grain boundaries with metal exfoliation, as was also found for other metals in same sites [16] and by other authors [21,22]. The mass loss was not only caused by metal anodic dissolution but also due to non-corroded grain detachment.

The aspect of a pickled sample exposed during 11 months at site 5 (Fig. 7d), evidences a much less deep attack penetration on Cu as compared to Al and its alloy 6201 [16].

As well as for Al and its alloy 6201 [16] in transverse cross-section heterogeneous distribution of the attack penetration along the circumference was also found probably associ-

ated to samples orientation respect to both pollutant sources and/or uneven TOW. This can be inferred from Fig. 7 for the most heavily polluted sites 5 and 9 after 4 and 11 month and sites 2 and 27 for 11 and 24 months exposure. Softer and more uniformly spatial distributed attacks were on the contrary observed on samples exposed to the lowest Cl^- content atmospheres, as those corresponding to Fig. 4a.

The Cu samples cross-section after each exposure period show two layered structure as was previously found for Zn and Al [17], Cu [18] and other metals as Fe [19]. According to EDX results on each SEM of corrosion product layers abundant soil contaminants were always involved for each site and exposure period. In this study an outer surface contamination layer was neither observed, as during outdoor corrosion tests [20–22] nor as referred by other authors [23].

The corrosion products formed are always insoluble in rain water copper compounds, as basic chlorides or sulphates, which also incorporate during the wet film growth soil elements as permanent contaminants.

The insoluble character in rain water prevents all pollutant elimination from the outer layer and their concentration at the metal corrosion product film interphase. Thus EDX analysis always reveals homogeneously distributed along the whole film thickness the presence of all the environmental pollutants of the test site.

4.3. Solid pollutants

Solid pollutants incorporated on wet corrosion products along the whole exposure time can be appreciated through SEM-EDX in plan as in cross-section analyses from the metal surface to the outer film surface. The presence of high Si, Al, Ca, Mg, Fe, Na, Zn and other soil elements through the whole corrosion product film thickness was found for every site and exposure period. As shown in Figs. 6 and 7 high proportion of spurious elements coming from the soil during outdoor test, are usually found during atmospheric corrosion studies.

They are also revealed by X-ray results, as shown in Table 2, and must also be bared in mind because these apparently inert components may act as crack and void filler in the corrosion product layers, improving film protectiveness. During some studies on the contrary, soil elements settled down on bare metals increase the TOW due to capillary or hygroscopic effect accelerating corrosion nucleation and increasing the Cl^- and/or SO_2 effect in polluted atmospheres [24].

4.4. Anomalous weight losses

Amongst the marine test stations, in the highest Cl^- polluted site 2 copper samples presented lower weight losses than at site 28 with less than 1/3 Cl^- and almost the same SO_2 content. According to Fig. 4 they are also below those from site 29, with lower Cl^- even in spite of higher SO_2 levels.

As in previous studies [17–19] corrosion products formed in some marine environments evidenced low weight losses, also revealing high protectiveness increase with time. This behavior obtained for Al and its alloy 6201 in these test sites [16], however does not apply to Cu samples, as can be inferred from Fig. 7c. In fact, polarisation in 0.1 M Na_2SO_4 electrolyte applied to samples retired from sites 2 and 27 after 24 month exposure was also intended on Cu waiting for the same behavior, but unexpectedly it resulted the opposite.

Even when Fig. 9 confirms through the high protectiveness of its corrosion product film with time that there must happen copper dissolution, with protective products film formation, the ESEM aspect shows that the weight loss must also involve loose grain detachment on the entire wire surface. Moreover, the polarisation results justify the exfoliation shown in Fig. 7c.

Copper weight loss as a function of time shown in Fig. 4 allows a careful analysis of each slope to evaluate the simultaneous effect of different pollutant proportions, allowing comparison among samples exposed at distinct sites for each period. But the pickling process is sometimes not efficiently performed when samples had been exposed to some atmospheric conditions provoking very increased corrosion product adherence respect to other sites simultaneously tested. The time needed for the complete removal can be considered a measure of the protectiveness they show on the underlying metal.

The results shown in Fig. 9a–c could be useful to predict the electricity transmission lines behavior in service, were they are simultaneously submitted to tensile strength caused by their own weight.

Best protectiveness would thus provide the longest useful life expectation.

4.5. Protectiveness of corrosion products

Always corrosion products led to corrosion rate decrease with respect to the initial bare metal as can be inferred from Figs. 8 and 9. Such decrease depends on the barrier effect due the corrosion products. The chemical composition and structure adopted by the corrosion product components determine the barrier layer efficiency in decreasing the corrosive agents access to the metal. Opposite to the observed on the same test sites for Al and its 6201 alloy [16], Cu shows a slight weight loss vs. time decrease with time after exposure at sites whit lowest [Cl^-] and various [SO_2], quite enhanced weight loss vs. time increase at sites with higher [Cl^-] than [SO_2], as can be seen comparing Fig. 4a and b for Al and its alloy with the homologous figures in copper. As a consequence, also the respective slopes of those figures, shown in Fig. 9a and b show remarkable differences amongst Al and Cu. For the highest [Cl^-] susceptibility of Cu it can also be appreciated a more intense protectiveness of the corrosion products formed, comparative fact frequently found for different metals exposed to the most aggressive atmospheres [17–19,24].

Corrosion rate vs. time provide once again experimental evidence of the unexpected inverse proportionality between metal weight loss by atmospheric corrosion and product film protectiveness. This was especially found in the presence of higher [Cl^-] than [SO_2] pollutant, as was also demonstrated for Al [16] in the most aggressive marine test site 2 as compared to site 27. This result however, was the opposite in this paper for Cu in the same marine sites, while Cu showed the said behavior comparing the respective marine-industrial sites in Figs. 5 and 9c.

Respect to these marine-industrial atmospheres the relative incidence of different [SO_2], samples exposed among sites 5 and 9, in Fig. 8, through electrochemical polarisation reveal higher protectiveness for the corrosion products film formed during 11 months at site 5 than 9.

The apparent [Cl^-] efficiency for increasing atmospheric corrosion of Cu is quite higher than that of [SO_2]. Comparing Figs. 4b and 5, for sites 27 and 10, for almost the same [Cl^-] the latter is slightly more corrosive on Cu than 27, even with 17 times higher [SO_2] in site 10; site 23 is in the same aggressiveness order as 24,12 and 15 in spite of having quite higher

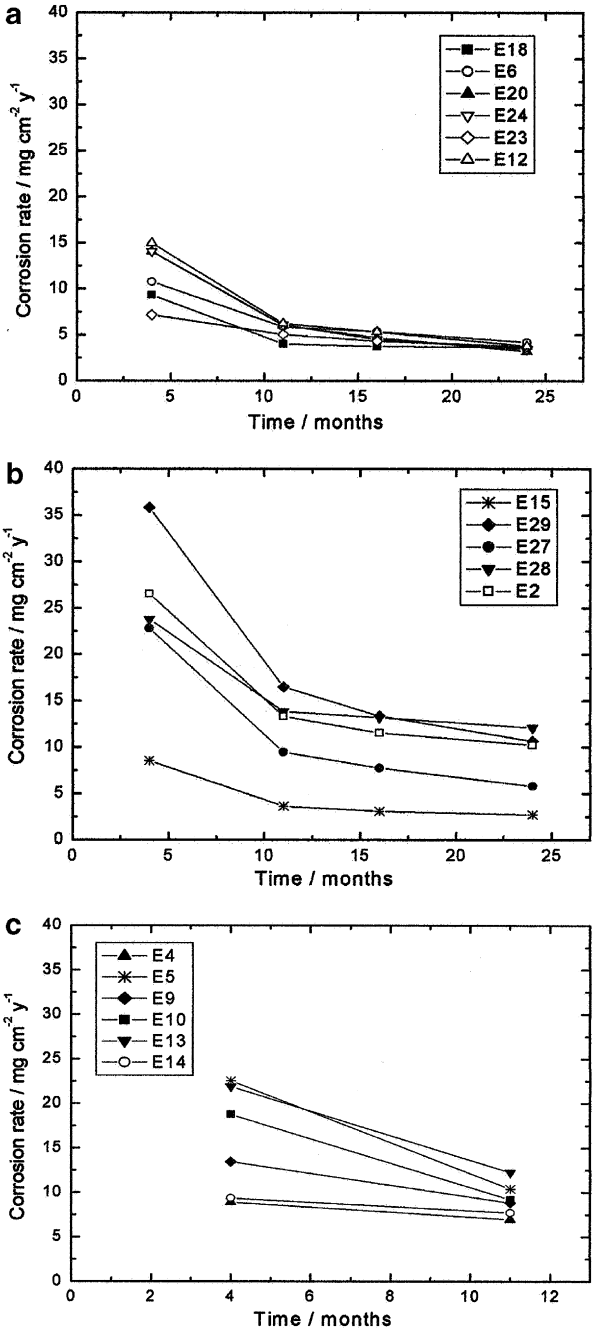

Fig. 9. Slope of graphs in Figs. 4 and 5 as a function of exposure time for copper in the different types of atmospheres: (a) Cu in marine sites 18, 6, 20, 24, 23 and 12, with lowest Cl^- and various SO_2 contents, (b) Cu in marine stations 15, 29, 28, 27 and 2, with higher Cl^- than SO_2 contents and (c) Cu in marine-industrial stations 10, 14, 4, 13, 9 and 5, with higher SO_2 than Cl^- contents.

[SO_2] than [Cl^-]; site 10 is quite more aggressive than 14 for a little higher [Cl^-] and almost the same total pollutant content.

However, it is very interesting to discuss the aspects to be considered to understand this very frequently confirmed mechanism [25–27] which could seem contradictory: in spite of Fig. 5, where higher Cu corrosion rates were determined at site 5 than 9, with similar [Cl^-] and more than twice [SO_2] in the first one, the protectiveness of the corrosion products film on copper, has the opposite trend for these most aggressive marine-industrial test sites, according to Figs. 8 and 9. From Fig. 7a and b the morphology and elemental film composition allow to correlate the exposed results.

4.6. Electrochemical analysis

Those most relevant data were investigated through electrochemical polarisation in 0.1 M Na_2SO_4 solution. Opposite to the behavior observed for aluminium [16] in $NaNO_3$, copper evidenced the contrary protectiveness when electrochemically investigated after 24 months exposure in same conditions, at the marine sites 2 and 27. Even when corrosion product protectiveness allowed explaining the lower corrosion rate found in site 2 than in 27 for Al, Cu corrosion products appeared to be more protective in site 27 than in 2, as shown in Fig. 8. Witness non-exposed copper samples evidenced the highest anodic and cathodic current densities and lower Ec, as well as for Al, due to their more susceptible original Al_2O_3 film and bare Cu surface, as compared to the barrier effect caused by the corrosion products formed in both sites.

The explanation can again be obtained from the structure aspect through ESEM comparative aspects shown in Fig. 7c. In fact, the thinner and cracked film and underlying exfoliation occurred at site 2, for the highest [Cl^-] atmosphere than for the one with 1/4 [Cl^-] of site 27, with almost the same [SO_2] may justify polarisation results.

Analogous comparison in 0.1 M Na_2SO_4 electrolyte, on the contrary demonstrated for copper in marine-industrial atmospheres that site 5 produced more protective corrosion product film than site 9, for more than twice [SO_2] and similar Cl^- contents.

More protective films were characterised by higher E_c and lower i_c than those for bare sample in both type of sites.

4.7. Evaluation of TOW effect

In a previous paper the TOW was the only parameter depending of the flat sample inclination in a marine environment of this Chilean region, being the cause for noticeable differences in the corrosion rate for different exposition angles [19].

The exposed wires conforming open helixes did not evidence the almost clear difference between sky and ground-ward surface observed in flat samples. All possible orientations and inclinations, on the contrary undergo uneven effect of pollutant deposition, washing-out by rains, sun drying, and almost uniform evaporation of dew by winds.

The TOW should not be considered an exclusive result of environmental conditions for liquid water condensation, as defined by ISO 9224 standard [11]. In previous studies in five test stations in Argentina it was demonstrated that estimations according to this standard were affected by up to yearly 400% error [24]. The metal on which water deposition occurs is determinant of its TOW, due to its colour, roughness, hygroscopic character of the surface, etc. Once corrosion initiated the surface properties of the metal enhance differences in

the capacity of liquid water retention, further precipitation, hydrolysis reactions etc, increasing the surface heterogeneities to bring even more scattered TOWs, locally enhancing differences in corrosion rate along the entire wire surface.

The low mean TOW of the whole region under atmospheric exposure, estimated in around 20%, following ISO 9224 standard [11], results in too high pollutant available to get them completely dissolved. This liquid water limitation does not fully allow manifesting the atmospheric contaminants content. The good correlation obtained for weight loss vs. the total pollutant levels, not only for each period but also over the whole exposure time, allows proposing a cooperative effect of pollutants, with very different effect for each of them, on different metals [16].

Previous results on steel [19] and on Al [16] yet revealed this restriction in the contaminants effect associated to low mean TOWs of this Chilean region, limiting the available liquid water to produce such highly concentrated electrolytes.

4.8. Analyses of the effect of Cl^- and SO_2 pollutant contents and other atmospheric parameters

As in a previous paper in the same test sites [16] the analysis of the corrosive effect of joint pollutants on copper weight loss was represented as a function of the total concentration for the 11 selected marine test sites after each exposure period in Fig. 10. The most relevant findings discussed are:

1. The already analysed low weight loss of pure copper in atmosphere 2. Other marine sites showed reasonable higher corrosion rates as a function of the total atmospheric pollutant concentration for all tested periods.

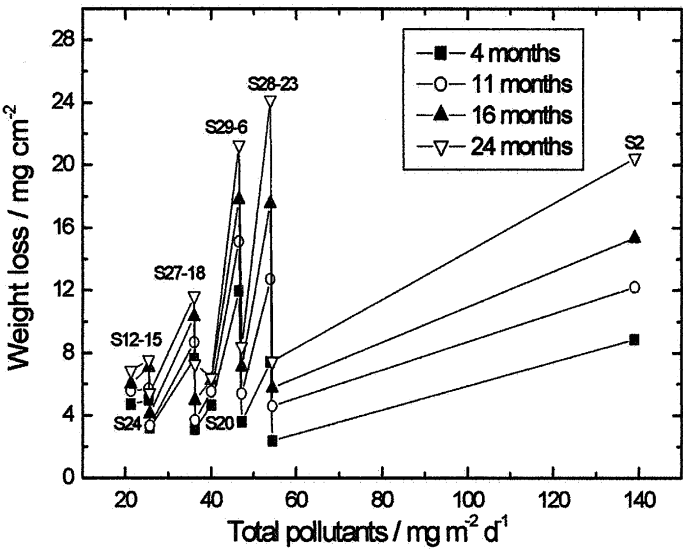

Fig. 10. Weight loss of copper in the 11 marine stations as a function of the total pollutant content of the test sites, for the 4 distinct exposure times.

2. As well as for Al and its 6201 alloy, but with very distinct magnitudes, sharp decreases were found at sites 15, 18, 6 and 23 after each of the 4 test periods for increasing total pollutants content. The corrosive effect of atmosphere would not only be determined by the pollutant content [16], but should also be proportional to the TOW, during which liquid water would permit enough salt dissolution to support electrochemical reactions enhancing corrosion. Increasing distances to the seashore line will cause TOWs decrease accordingly diminishing metal weight loss at the respective test site. Thus, most abrupt weight loss decrease must be expected, and it was in fact measured, for stations located at longer distances from the sea than their 2 adjacent, as 24, 15, 18, 20, 6 and 23, in decreasing order.
3. Respect the height over sea level, a factor recovering for long distance the marine fog effect, it allows on the contrary, less condensation barriers such as trees or buildings, allowing salt and TOWs increases due to SW predominant winds from the sea. This would increase metal weight losses in sites 15, 20, 29 and 23, as were also determined for Al and its 6201 alloy samples [16].

According to Fig. 11, deviation in weight loss duplicate data, limits further exploitation of the displayed results.

Similar analysis was not intended for samples exposed in the marine-industrial test sites, because as all of them are nearer to the sea shore line and at more uniform heights over sea level, less evident TOW differences could be inferred. Also, the much higher SO_2 as compared to the Cl^- contents with higher dew condensation relative to the various marine sites would not originate such aggressiveness scattering in the pollutants effect. However the distance to the sea shore seems to evidence a more clear effect on weight losses than the SO_2 content in these atmospheres.

Previous results on Al [16] for these 6 sites respect to the TOWs on the metallic samples suggested a probable more efficient dissolution of the available pollutants, based on the higher maximum weight losses determined for Al and the alloy sample as compared to the

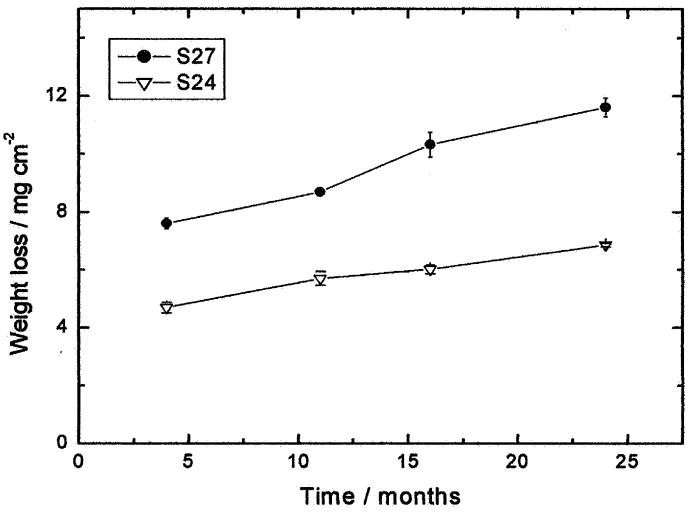

Fig. 11. Weight loss deviation of copper in marine stations 24 and 27.

11 marine test sites. This evidence of a corrosive effect by water dissolution of both pollutants additional to higher SO_2 levels manifested in all these sites could be applied to discuss the data obtained for Cu samples.

According to previous results for Al, in all the marine atmospheres an additional effect on weight losses seemed to result of the total pollutants, producing a rather cooperative, than competitive or synergic effect on both metals. However, the present results for Cu show an opposite behavior in the marine atmospheres with low Cl^- contents and in these marine-industrial test sites. In both of them unexpected low weight losses were determined, discarding a synergic or cooperative effect of both pollutants as suggested on the basis of Al and its alloy results. The most probable interaction seem to preferably reflect a competitive effect of the same pollutants, during parallel tests performed simultaneously with all metals.

However, the results exposed in Fig. 10 evidence that the pollutant interaction is more strongly determined by the tested metal.

5. Conclusions

The results produced a new approach on copper atmospheric corrosion, as a function of samples exposure time, characteristic morphology and protectiveness of product films and the combined effect of most abundant pollutants and frequent environmental parameters.

1. Copper samples exposed to marine sites with the lowest Cl^- contents produced very low weight losses, especially as compared to Al and its alloy.
2. In the marine test sites with higher $[Cl^-]$ than $[SO_2]$ the weight losses vs. time increase reveals the stronger corrosive effect of the first pollutant.
3. At the marine-industrial sites, Cu showed very low corrosion rates for Cl^- contents in the order of the those measured in the lowest $[Cl^-]$ marine sites, in spite of much higher SO_2 contents.
4. The limitation in the corrosion rates depicted in conclusions 1–3 can be attributed to highly protective product films formed by effect of the respective atmospheric $[Cl^-]$, except for its excessive content in site 2.
5. These results would reproduce the first steps and short time atmospheric effects, responsible for traditional long lasting patina.
6. Life expectancy seems to be higher for copper wires in marine than in marine-industrial test sites, also as compared to the Al alloy 6201.
7. Corrosion products protectiveness showed the maximum increase during first to the second exposure period.

Acknowledgements

Chilquinta Energía and the Research Management of the Pontificia Universidad Católica de Valparaíso, Chile, financially supported this research project.

References

[1] M. Morcillo, E. Almeida, M. Marrocos, B. Resales, Corrosion 57 (11) (2001) 967–980.
[2] I.T.E. Fonseca, R. Picciochi, M.H. Mendonca, A.C. Ramos, Corros. Sci. 46 (2004) 547–561.
[3] K. Nassau, P.K. Gallagher, A.E. Miller, T.E. Graedel, Corros. Sci. 27 (7) (1987) 648–669.

[4] K. Nassau, A.E. Miller, T.E. Graedel, Corros. Sci. 27 (7) (1987) 703–719.
[5] R.L. Opila, Corros. Sci. 27 (7) (1987) 685–694.
[6] X. Zhang, W. He, I. Odnevall, J. Pan, C. Leygraf, Corros. Sci. 44 (2002) 2131–2151.
[7] M. Watanabe, Y. Higashi, T. Tanaka, Corros. Sci. 45 (2003) 1439–1453.
[8] A. Leuenberger-Minger, B. Buchmann, M. Faller, P. Richner, M. Zobeli, Corros. Sci. 44 (2002) 675–687.
[9] Private experience and communication during ISOCORRAG project, ISO 1988–98.
[10] ISO 9223, Corrosion of metals and alloys, Classification of corrosivity of atmospheres, ISO, Geneva, 1991.
[11] ISO 9224, Corrosion of metals and alloys, Guiding values for the corrosivity categories of atmospheres, ISO, Geneva, 1991.
[12] ISO 9225, Corrosion of metals and alloys, Corrosivity of atmospheres – methods of measurement of pollution, ISO, Geneva, 1991.
[13] ISO 9226, Corrosion of metals and alloys, Corrosivity of atmospheres – methods of determination of corrosion rate of standard specimens for the evaluation of corrosivity, ISO, Geneva, 1991.
[14] ISO 8407, Metal and alloys – procedures for removal of corrosion products from corrosion test specimens, ISO, Geneva, 1992.
[15] K.S. Rajagopalan, S. Chandrasekaran, M. Sundaram, P.S. Mohan, Proc. 5th Int. Symposium on Modelling on Environmental Effects on Electrical and General Engineering Equipment, Liblice, 1978, pp. 183–193.
[16] R. Vera, D. Delgado, B. Resales, Part 1, Corros. Sci. 48 (2006) 2882–2900.
[17] J.R. Vilche, F.E. Varela, G. Acuña, E. Codaro, B.M. Resales, A. Fernández, G. Moriena, Corros. Sci. 37 (6) (1995) 941–961.
[18] J.R. Vilche, F.E. Varela, G. Acuña, E. Codaro, B.M. Resales, A. Fernández, G. Moriena, Corros. Sci. 39 (4) (1997) 655–679.
[19] R. Vera, B.M. Resales, C. Tapia, Corros. Sci. 45 (2003) 321–337.
[20] J. Hitzig, K. Jüttner, W.J. Lorenz, W. Paatsch, Corros. Sci. 24 (1984) 945.
[21] F. Mansfeld, M.W. Kendig, J. Electrochem. Soc. 135 (1988) 828.
[22] K. Jüttner, W.J. Lorenz, W. Paatsch, Corros. Sci. 29 (1989) 279.
[23] T.E. Graedel, J. Electrochem. Soc. 136 (1989) 204.
[24] B.M. Rosales, Maps of Atmospheric Corrosiveness of Argentina, first ed., América Editora, Buenos Aires, 1997, p. 189–192.
[25] J. Richter, H. Kaesche, Werk. Korros. 32 (1981) 174.
[26] G.C. Wood, J.A. Richardson, M.F. Abd Rabbo, L.P. Mapa, W.H. Sutton, in: R.P. Frankental, J.P. Kruger (Eds.), Passivity of Metals, The Electrochemical Society, Princeton, 1978.
[27] M. Morcillo, E. Almeida, B. Rosales, J. Uruchurtu, M. Marrocos, Corrosion and protection of metals in the atmospheres of Ibero-America, Part 1, CYTED, Madrid, 1998, p. 588.